

PCCP

Accepted Manuscript



This is an *Accepted Manuscript*, which has been through the Royal Society of Chemistry peer review process and has been accepted for publication.

Accepted Manuscripts are published online shortly after acceptance, before technical editing, formatting and proof reading. Using this free service, authors can make their results available to the community, in citable form, before we publish the edited article. We will replace this *Accepted Manuscript* with the edited and formatted *Advance Article* as soon as it is available.

You can find more information about *Accepted Manuscripts* in the [Information for Authors](#).

Please note that technical editing may introduce minor changes to the text and/or graphics, which may alter content. The journal's standard [Terms & Conditions](#) and the [Ethical guidelines](#) still apply. In no event shall the Royal Society of Chemistry be held responsible for any errors or omissions in this *Accepted Manuscript* or any consequences arising from the use of any information it contains.

Cite this: DOI: 10.1039/c0xx00000x

www.rsc.org/pccp

PAPER

The effects of counterion composition on the rheological and conductive properties of mono- and diphosphonium ionic liquids†

Reimi Yonekura^a and Mark W. Grinstaff^{*b}

Received (in XXX, XXX) Xth XXXXXXXXX 20XX, Accepted Xth XXXXXXXXX 20XX

DOI: 10.1039/b000000x

A series of monocationic and dicationic phosphonium ionic liquids was prepared and their thermal, rheological, and conductive properties were characterized. These phosphonium ionic liquids were paired with seven monoanionic counterions (chloride, hexafluorophosphate, hexafluoroantimonate, octanoate, perfluorooctanoate, dodecyl sulfate, dioctyl sulfosuccinate, and bis(trifluoromethane)sulfonimide) in order to examine the effects of the counterion size and chemical structure on bulk properties of the phosphonium ionic liquids. The length of the three alkyl chains surrounding the phosphorus atom was also varied from butyl, hexyl to octyl on the cation. All of the samples exhibited initial decomposition temperatures above 150 °C. The octanoate and its fluorinated analog possessed the lowest decomposition temperature and the dicationic hexyl sample bis(trifluoromethane)sulfonimide possessed the highest (> 370 °C). The dicationic butyl and hexyl chloride samples displayed similar G' , G'' and viscosity curves, whereas the dicationic octyl chloride sample exhibited significantly lower values. The frequency sweeps of the monocationic phosphonium ionic liquids were all similar and showed minimal side chain dependence. The monocationic phosphonium ionic liquids have higher conductivity than their dicationic analogs at all measured temperatures.

Introduction

Ionic liquids (ILs) are mixtures of compounds consisting of only ions, and, typically, possess melting temperatures below 100°C.¹⁻⁸ Classification of ILs is usually based on the cation present in the system. The ILs often described in the literature are the imidazolium, pyridinium, pyrrolidinium, and alkylammonium-based ILs. The corresponding counterions are usually singly charged inorganic or organic ions, and range from simple halides (e.g., Cl⁻) to multi-atom species such as bis(trifluoromethane)sulfonamide, NTf₂⁻. Recently, the pairing of multicationic ILs with single and multiple charged anions were also reported as a means to prepare functional ionic self-assemblies.⁹⁻¹¹

Applications for ILs span from lubricants to solvents for chemical reaction processes. As a material composed of charged species, ILs are investigated as electrolyte solvents for lithium or

sodium ion batteries, supercapacitors, and fuel cells. For example, Sakaebe reported a quaternary ammonium-based ionic liquid for use in a Li/LiCoO₂ cell that maintained a specific capacity above 110 mAh/g even after 30 cycles at a C/10 current rate.¹² Liu *et al.* successfully prepared a supercapacitor with an MnO₂ nanocomposite positive electrode with an activated carbon negative electrode and imidazolium-based ionic liquid/dimethylformamide electrolyte with superior energy density (78.4 Wh/kg) and power (12.7 kW/kg).¹³ Immobilizing imidazolium-based ILs in polymer membranes also affords a water-free system for fuel cells that currently use humidity-dependent membranes.¹⁴⁻¹⁶ In addition, electrochemical deposition of metals, such as aluminum, that require temperatures above 100 °C are now possible using imidazolium-based ILs.¹⁷ For these aforementioned applications and the continued investigation of this area, it is critical to investigate relationships between structure, property and performance for key ionic liquid characteristics such as thermal stability, rheology, and conductivity.

Several reports describe some of these critical relationships and trends for monocationic ILs.¹⁸⁻²⁵ Generally, attaching long or bulky hydrocarbons to the central atom of the cation results in lower melting temperatures. The Seddon group described monocationic alkylphosphonium halide species, where varying the fourth alkyl chain around a trioctyl follows this trend from methyl to propyl chain lengths while the tributyl equivalent system does not.^{18, 19} Brennecke showed with imidazolium ILs

^aDepartment of Mechanical Engineering, Boston University, Boston, Massachusetts 02215, United States

^bDepartments of Chemistry and Biomedical Engineering, Boston University, Boston, Massachusetts 02215, United States. E-mail: mgrin@bu.edu; Fax: +1 617 358 3186; Tel: +1 617 358 3429

†Electronic supplementary information (ESI) available: (1) Tabulated summary of physical and chemical properties of the phosphonium ILs; (2) graphs of frequency sweeps of investigated ILs; (3) tabulated NMR data, TGA data, and conductivity data of all ILs presented. See DOI: 10.1039/b000000x/

that as the hydrocarbon chain length increases from ethyl to butyl on the cation, their glass transition, crystallization, and melting temperatures increase.²⁰ With a thiocyanate counter ion, pyrrolidinium ILs show a decreasing melting point trend with increasing alkyl chain length on the cation.²¹ Melting temperature can also be controlled by varying the anion size as well as introducing anions such as thiocyanate and dichloroacetate. This agrees with Seddon *et al.*'s findings with the phosphonium cationic ILs where larger halides increase the interionic distances and the packing efficiency, leading to higher melting points.¹⁹ With a larger anion, the thermal stability also increases. Exchanging the imidazolium-based ionic liquid to a phosphonium analogue while maintaining the same anion, increases the viscosity up to eight times.²² However, the melting temperatures of phosphonium ILs are higher than that of their imidazolium analogs, 25 and -26 °C respectively for the two species with a dodecane linkage chain.

Relevant reports on dicationic ILs were published by the Armstrong Lab.^{26, 27} Variations of imidazolium and pyrrolidinium-based cation ILs or cations with combinations of imidazolium, ammonium, pyridinium, pyrrolidinium, and phosphonium moieties to make asymmetric dications with common anions are discussed. They found that increasing the alkyl chain length on imidazolium-based dications decreases the melting temperature of the whole system as a result of higher degrees of conformational freedom. The anion choice also affects the thermal properties with larger anions, such as NTf₂⁻, preventing efficient packing of the ions and weakening ion-ion interactions, resulting in lower melting temperatures compared to the halide analogs. Extending this work to include the complexations of a dicationic IL with tetraanions and polyanions, the compositions formed between diphosphonium cations and ethylenediaminetetraacetic acid (EDTA), porphyrin, or polyacrylic acid are recently reported.^{9, 11} For example, when the dication 1,10-di(trihexylphosphonium)decane, which was originally paired with two monoanion chloride counter ions, is now paired with the EDTA tetraanion, a significant increase in viscosity is observed as a consequence of a network formation. A polymeric network can only be formed between 1,10-di(trihexylphosphonium)decane and poly (acrylic acid) (MW: 100 000 g/mol) while only a mixture can be formed from mixing the monocationic equivalent, 1-trihexylphosphonium decane, and poly (acrylic acid). The ionic polymeric network exhibits thermal and mechanical reversibility along with a high viscosity at room temperature. A polystyrene phosphonium polymer is recently reported that upon coordination with monoanions (stearate, oleate, and 15-oxo-2,5,8,11,14-pentaoxaoctadecan-18-oate or a dianion (dodecanedioate) forms supermolecular ionic materials that are highly ductile, or brittle and transparent, respectively, based on the coordinated anion.²⁸

Despite the significant work that has been done on ILs, opportunities still exist to prepare specific cation and anion combinations, to study their properties, and to optimize their properties via a systematic study for an intended application. It is known that phosphorous-based ILs can be more thermally stable than nitrogen-based ILs,²⁹ hence phosphonium systems were selected to address the increasing applications that require thermally robust IL solvents; specifically, electrolyte solvents for

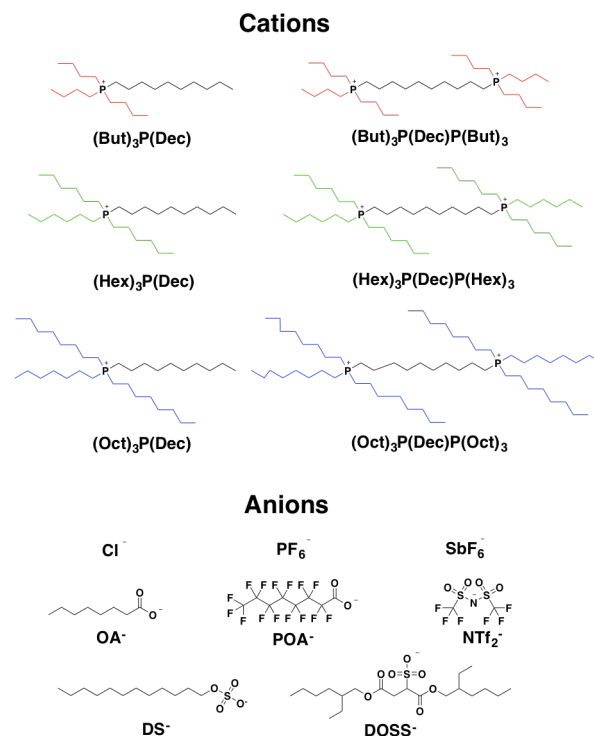


Figure 1. Monocationic and dicationic alkyl phosphonium ILs with various anions including: chloride Cl⁻, hexafluorophosphate PF₆⁻, hexafluoroantimonate SbF₆⁻, octanoate OA⁻, perfluorooctanoate POA⁻, dodecyl sulfate DS⁻, dioctyl sulfosuccinate DOSS⁻, and bis(trifluoromethane)sulfonimide NTf₂⁻.

batteries used in the automotive, oil and gas recovery, and manufacturing industries with operating conditions between 75 and 150 °C. In this manuscript, we present a library of monocationic and dicationic phosphonium-based ILs, paired with a variety of structurally and electronically different monoanions (Figure 1). The bulk properties were characterized using rheometry, thermal analysis, and conductivity.

Results and discussion

Synthesis

The monocationic and dicationic phosphonium chloride ILs were prepared following reported procedures.² The substitution of the chloride anion with hexafluorophosphate, hexafluoroantimonate, octanoate, perfluorooctanoate, dodecyl sulfate, dioctyl sulfosuccinate, or bis(trifluoromethane)sulfonimide was performed using a standard salt anion exchange. Specifically, [(Hex)₃P(Dec)P(Dec)₃] was paired with PF₆⁻, SbF₆⁻, NTf₂⁻, and POA⁻. The [(But)₃P(Dec)P(Dec)₃] was paired with OA⁻, POA⁻, DS⁻, and DOSS⁻. The octanoate was included as a comparison for the perfluorooctanoate. For clarity and discussion in the text, the phosphonium ILs are referred to by number (PIL#, Table 1) with the monocationic phosphonium ILs being PIL1-3 and the dicationic phosphonium ILs being PIL4-14. The name for the phosphonium cations derives from the length of the alkyl chains surrounding the phosphorous atoms. A short form is adopted with

Table 1. Physical and chemical properties of the phosphonium ILs

PIL/Entry	Ionic liquid	MW (g/mol)	T _m (°C)	T _d (°C)	Viscosity Pa.s (1 Hz, 25 °C)
1	[(But) ₃ P(Dec)](Cl)	379.05	N/A	302, 367	5.05
2	[(Hex) ₃ P(Dec)](Cl)	427.76	N/A	277, 351	2.49
3	[(Oct) ₃ P(Dec)](Cl)	511.92	N/A	283, 351	2.53
4	[(But) ₃ P(Dec)P(But) ₃](Cl) ₂	615.8	87	321, 397	3.88x10 ⁵
5	[(Hex) ₃ P(Dec)P(Hex) ₃](Cl) ₂	784.1	43	298, 380	2.64x10 ⁵
6	[(Oct) ₃ P(Dec)P(Oct) ₃](Cl) ₂	952.5	N/A	288, 370	2.63x10
7	[(Hex) ₃ P(Dec)P(Hex) ₃](PF ₆) ₂	1003.2	N/A	302, 370	2.01x10
8	[(Hex) ₃ P(Dec)P(Hex) ₃](SbF ₆) ₂	1184.8	N/A	324, 391	1.46x10
9	[(Hex) ₃ P(Dec)P(Hex) ₃](POA) ₂	1540.1	N/A	165, 267	1.15x10
10	[(Hex) ₃ P(Dec)P(Hex) ₃](NTf ₂) ₂	1274.4	N/A	375, 542	2.0
11	[(But) ₃ P(Dec)P(But) ₃](OA) ₂	831.3	N/A	156, 346, 366	4.65x10
12	[(But) ₃ P(Dec)P(But) ₃](POA) ₂	1371	N/A	155, 257, 461	1.34x10
13	[(But) ₃ P(Dec)P(But) ₃](DS) ₂	1075.7	173 (T _c)	254, 482	1.61x10
14	[(But) ₃ P(Dec)P(But) ₃](DOSS) ₂	1388.1	N/A	278, 469	2.23x10
	Na ⁺ DOSS ⁻	444.56	N/A	260.42	
	POAH *	414.07	55	78.28	
	SDS *	288.38	206	203.28	

The material properties of the starting materials have been included for reference. Crystallization temperature (T_c), and melting temperature (T_m) were measured using DSC. Decomposition temperature (T_d) was measured using TGA and viscosity values were obtained from rheometrical data at 1 Hz.

a number designating the number of positive charges on the cation (1 or 2) followed by the length of the side alkyl chain (But, Hex, Oct). As all of the cations have a central alkyl chain that contains 10 carbon atoms in length, this description is omitted in the short hand form. For reference, structures of the cations and anions under study are shown in Figure 1.

Thermal properties

The differential scanning calorimetry (DSC) results show minimal variation in thermal properties between the monocationic ILs PIL1, PIL2, and PIL3 unlike their dicationic equivalents PIL4, PIL5 and PIL6, which vary greatly for both glass transition temperature (T_g) and melting temperature (T_m) as shown in Figure 2 and Table 1. For the monocationic ILs, a slightly larger T_g value (≈6 °C) was observed for PIL1 (-56 °C) compared to PIL3 (-62 °C) and PIL2 (-63 °C). This may be attributed to the shorter alkyl chains of the butyl ILs enabling a stronger electrostatic interaction between the phosphonium cation and the chloride anion. The T_g values for PIL2 and PIL3 were not significantly different, indicating that once the alkyl chains were longer than six carbons in length, the T_g was insensitive to the compositional change around the phosphorus atom. Seddon also saw minimal T_g differences between their alkyl-imidazolium systems with butyl to nonyl alkyl chain lengths.³⁰ The PIL4, PIL5, and PIL6 dicationic ILs all had T_g values higher than their respective monocationic analogs (-22, -51, and -54 °C respectively). This suggests that the dicationic ILs possess

a more ordered structure below the glass transition temperature. The PIL4 and PIL5 ILs solidified at room temperature and subsequently had a measurable T_m of 87 and 43 °C, respectively (Table 1, entries 4 and 5). The dependence of T_m on the alkyl side chain length surrounding the phosphonium cation is significant, as the T_m of PIL4 is approximately twice that of the PIL5. The increase in steric hinderance due to the longer hexyl chains of PIL5 reduces the electrostatic interaction between the phosphonium cation and the chloride anion as well as inhibits ordered packing of the material. No T_m was observed for PIL6 between -70 and 150 °C when the alkyl chain length is extended to eight carbons around the phosphonium cation and for the three monophosphonium ILs: PIL1, PIL2, and PIL3.

The ILs presented in this study have multiple decompositions temperatures (T_d). This has been observed in other phosphonium systems.^{6, 31} With regards to the decomposition mechanism of phosphonium ILs, Stevens *et al.*, Keating *et al.*, and Calado *et al.* reported that a reverse Menshutkin reaction occurs where an alkylchloride chain, phosphine, and some phosphorous oxide are produced after the first decomposition step.^{6, 31, 32} All of the monocationic and dicationic phosphonium chloride ILs have high first T_d values between 155 and 321 °C, with the second T_d occurring about 70-80 °C higher (Table 1 entries 1, 2, 3, 4, 5, and 6 and see SI, Figure SI5). The phosphonium cations paired with the POA or OA anion possess the lowest T_d (PIL9, PIL11, and PIL12, 155-165 °C), while all the other phosphonium ILs possess a first T_d > 277 °C. The dicationic chloride ILs exhibited a slight

decrease in both decomposition temperatures with an increase in the alkyl chain length surrounding the phosphonium cation (Table 1, entries 4, 5, and 6). This behavior was not observed for the first decomposition step of the monocationic chloride ILs. A slight decrease in the second decomposition temperature was observed when going from the PIL1 to PIL2 but not between PIL3 and PIL2.

Next we investigated the effect of exchanging the anion from a chloride to a larger anion such as PF_6^- , SbF_6^- , POA^- , and NTf_2^- . We selected the PIL5 as the prototypical IL because the hexyl chain is the longest side chain that will produce an IL with a relatively high viscosity (η), for the forthcoming studies. The substitution of the chloride in PIL5 ($T_g = -51^\circ\text{C}$) with PF_6^- , SbF_6^- , or POA^- afforded a minimal change in the T_g (PIL7, PIL8, and PIL9, -50.6, -50, and -48°C respectively). The dominating factor for the glass-like to rubber-like transition when the counter ions are multiatomic is the cation present. The T_g was the lowest for PIL10 (-68°C) and likely reflects the relatively weak electrostatic interaction between the cationic phosphonium and the NTf_2^- anion, due to the delocalization of the negative charge in the anion (Figure 2). Similar to the cation dependence of T_g to the hexyl species presented above, the reduced steric congestion surrounding the phosphonium atom when comparing the cation in PIL9 to the cation in PIL12 results in an increase in T_g from -48 to -13°C . Unlike PIL5, PIL7, PIL8, PIL9, and PIL10 did not exhibit a T_m transition (Table 1, entries 7, 8, 9, and 10). This can be attributed to these anions being too large to pack with the phosphorous atom for solidification due to the steric hindrance of the side hexyl alkyl chains as well as weak electrostatic interactions with the phosphonium cation as compared to the chloride analog. For instance, the van der Waals radius of Cl^- , PF_6^- , and SbF_6^- are 0.181 nm, 0.259 nm, and 0.277 nm respectively.

The decomposition temperatures values were relatively insensitive to the coordinated anion for PIL5, PIL7, and PIL8 (See SI, Figure SI5). The PF_6^- and SbF_6^- salts have poor hydrolytic stability but should be more thermally stable than halides.³³⁻³⁵ When combined with the phosphonium cation the effect may have been dampened unlike the amplified effect seen with imidazolium based cations such as 1-Butyl-3-methylimidazolium [bmim] and (1-ethylpropyl)-methylimidazolium [eC₃mim].³⁶ The SbF_6^- anion is known to be more thermally stable than PF_6^- thus, the slightly higher first and second T_d values of the former is expected.^{37, 38} PIL10 had the highest thermal stability as compared to the other dicationic hexyl ILs (See SI, Figure SI5). A follow up experiment where this IL was subjected to 200 cycles of -70°C to 200°C ramp and then tested for thermal stability showed a 40°C decrease in T_d . Based on their thermal properties, PIL8 and PIL10 are the preferred choices, for use in electrochemical devices where thermal stability at elevated temperatures is necessary.

Given the trends observed for $[(\text{Hex})_3\text{P}(\text{Dec})\text{P}(\text{Hex})_3]$ coordinated with various inorganic anions, we next examined the effect of changing the counterion of $[(\text{But})_3\text{P}(\text{Dec})\text{P}(\text{But})_3]$ from Cl^- to larger hydrocarbons and fluorocarbons. As PIL4 had displayed the largest T_m among the dicationic chloride samples, differences in bulk properties that may arise from exchanging the halide with large anions were hypothesized to be more

pronounced. Unlike the chloride salt IL which is a solid, PIL12, PIL13, and PIL14 were liquids at room temperature (Table 1 entries 12, 13, and 14).

The T_g values for these ILs decrease in the following order: PIL12 $[(\text{But})_3\text{P}(\text{Dec})\text{P}(\text{But})_3](\text{POA})_2$, PIL13 $[(\text{But})_3\text{P}(\text{Dec})\text{P}(\text{But})_3](\text{DS})_2$, PIL14 $[(\text{But})_3\text{P}(\text{Dec})\text{P}(\text{But})_3](\text{DOSS})_2$, and PIL11 $[(\text{But})_3\text{P}(\text{Dec})\text{P}(\text{But})_3](\text{OA})_2$ (Figure 2). The T_g of $[(\text{But})_3\text{P}(\text{Dec})\text{P}(\text{But})_3](\text{Cl})_2$ or PIL4 (-22°C) is in between $[(\text{But})_3\text{P}(\text{Dec})\text{P}(\text{But})_3](\text{POA})_2$ PIL12 (-13°C) and $[(\text{But})_3\text{P}(\text{Dec})\text{P}(\text{But})_3](\text{DS})_2$ PIL13 (-42°C). Replacing the OA^- in $[(\text{But})_3\text{P}(\text{Dec})\text{P}(\text{But})_3](\text{OA})_2$ with the fluorinated analog POA^- increased the T_g value by -65°C to -13°C . As such, more energy is required for the POA^- phosphonium salt or PIL12 to transition to the amorphous, rubbery state. This stabilizing effect of the POA^- is seen for both dicationic butyl and hexyl ILs with the former IL achieving a higher T_g value (-13°C and -48°C respectively). Exchanging the OA^- for DS^- in the $[(\text{But})_3\text{P}(\text{Dec})\text{P}(\text{But})_3]$ results in an increase in the T_g by approximately -65°C to -42°C . This increase is due to the introduction of the sulfate group instead of the lengthening of the alkyl chain in the anion as $[(\text{But})_3\text{P}(\text{Dec})\text{P}(\text{But})_3]$ with a dodecane counter ion ($[(\text{But})_3\text{P}(\text{Dec})\text{P}(\text{But})_3](\text{DA})_2$) has a T_g of -70°C . Maintaining the sulfate coordination to the $[(\text{But})_3\text{P}(\text{Dec})\text{P}(\text{But})_3]$ but increasing the steric bulk around the sulfate anion via branched alkyl chains, using the DOSS anion (PIL14), affords an approximately 20°C decrease in the higher T_g value to -60°C .

The results from the thermal gravimetric analysis showed

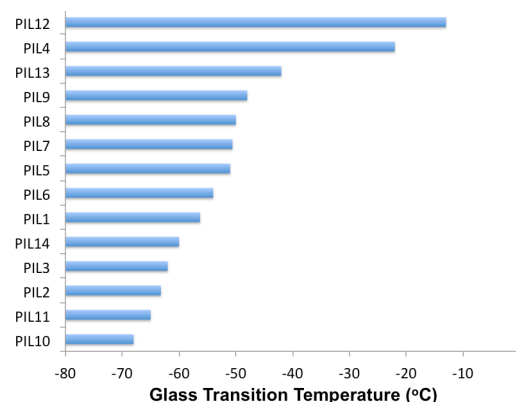


Figure 2. Glass transition (T_g) temperatures as measured by DSC for phosphonium ionic liquids.

lower thermal stability for larger anions as compared to the chloride salts (See SI, Figure SI5). In particular, PIL12 and PIL11 begin to decompose at half the temperature of the first step transition of the chloride equivalent. This trend is also seen in the T_d value for PIL9. This may stem from the low T_d of perfluorooctanoic acid (POAH , 78°C), the starting material for both PIL9 and PIL12. The lower thermal stability of ILs containing OA^- have been previously reported in literature when paired with other cations.^{39, 40} While PIL4 has two T_d 's, the fluorinated and non-fluorinated OA have an additional third T_d , which occurs at a much higher temperature for PIL12, compared to PIL11. While the first decomposition temperature is lower than that of PIL4, PIL13 and PIL14 possess a higher second decomposition step, which is likely due to the presence of the

sulfate group stabilizing the phosphine that decomposes in the second step. The DOSS⁺ analog (PIL14) has the highest initial decomposition temperature among the multiatomic butyl system but the subsequent decomposition occurs at an average temperature relative to the other non-halide anion systems (Table 1 entry 14 and see SI, Figure S15).

Rheological properties

Small differences in the viscosity, storage modulus (G'), loss modulus (G''), and phase angle (δ) properties, as measured by frequency sweeps, are observed between the monocationic chloride ILs PIL1, PIL2, and PIL3 (Figure 3 for viscosity and storage modulus data, and see SI, Figure S12). PIL1 possesses a slightly higher complex viscosity (η^*) than the hexyl and octyl analogs at all frequency values (0.1 to 100 rad/s). The G' frequency values for PIL1 and PIL2 exponentially increase with increasing frequency unlike the near linear response for PIL3 (See SI, Figure S12). PIL1 maintains a slightly higher value for G'' and η throughout the experiment than those with the longer side alkyl chains. The G' for PIL3 has a linearly increasing trend while PIL1 and PIL2 have a steady G' value at low frequencies which increases slightly above 1 rad/s. For the three monocationic ILs, G'' is consistently larger than the G' values between 0.1 rad/s and 100 rad/s (See SI, Figure S12).

All the monocationic chloride ILs maintain a δ of 90 degrees throughout the frequency sweep and no alkyl side chain length dependence is observed (See SI, Figure S12). These results are consistent with the low T_g values observed for these ILs as a consequence of the steric shielding caused by the three butyl, hexyl or octyl chains along with the ten carbon alkyl chain attached to the phosphorous of the cation.

Similar to the δ data, the η^* is not frequency dependent for the three monocationic ILs PIL1, PIL2, and PIL3 (See SI, Figure S12). η^* values range from 2.5 - 5.0 Pa.s at 1 Hz (6.28 rad/s), and where similar to those observed with dicationic imidazolium ILs bearing a bromide cation.²⁶ Based on the constant 90 degrees δ observed, this ideal Newtonian liquid behavior of the monocationic ILs is expected. The PIL1 possesses a slightly higher η^* than the PIL2 and PIL3 ILs due to the reduced steric hindrance from the alkyl side chains again. In the butyl analog, the positively charged phosphonium core is less shielded from the chloride anions than in the hexyl and octyl analogs.

The frequency sweeps for the dicationic ILs display a different behavior than their monocationic equivalents. The moduli and viscosities are magnitudes higher for the dicationic ILs and only PIL6 displays ideal viscous δ behavior similar to the monocationic ILs. Results from the frequency sweep performed on PIL4, PIL5, and PIL6 show alkyl side chain length dependence (See SI, Figure S11). The G' and G'' values increase with higher frequencies for all three dicationic ILs. G' and G'' are the real and imaginary components of the complex (rigidity) modulus (G^*) which captures the ratio between the complex shear stress and complex shear strain, implying that the degree of deformation of the ILs is smaller when shear strain is applied for a shorter period of time. In terms of the modulus dependence on the alkyl side chain length, a carbon chain longer than six carbons leads to a dramatic decrease in the moduli. When comparing the modulus values at 1 rad/s, PIL6 had G' and G'' values of 10^{-5} less

than the other two dicationic hexyl and butyl IL analogs (PIL4 & PIL5) and is more sensitive to the frequency change. The difference in length of the alkyl side chain of PIL4 and PIL5 does not affect G' and G'' . The frequency dependence of both moduli is non-linear unlike the octyl analog, PIL6. The G'' , δ , and η curves for PIL6 are similar to the monocationic ILs with a linear,

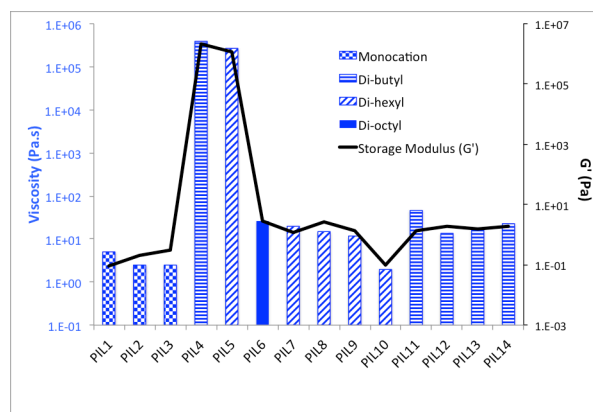


Figure 3. Viscosity and G' values recorded at 1 Hz for the monocationic and dicationic phosphonium ionic liquids.

positive curve for the first property and linear with no dependence on frequency for the latter two properties.

It is interesting to note that although PIL4 and PIL5 show frequency dependence for both of their moduli, only a mild dependence is seen in the δ graph (See SI, Figure S11). However, δ for both ILs never surpasses that of PIL6 and the monocationic ILs at all frequency values measured. The overall electrostatic interaction increases from the monocationic to dicationic ILs due to the gain in symmetry of ILs with the two phosphorus atoms and identical alkyl chains and the gain in charge per cation. The alkyl side chain length of eight carbons in PIL6 causes enough steric hindrance despite the increase in electrostatic interaction compared to the monocationic analog. This hindrance produces vastly lower moduli and η values and higher δ than the other two dicationic ILs. The tangent of δ captures the ratio between G'' and G' . In both PIL4 and PIL6, the two moduli were increasing at the same rate with frequency (See SI, Figure S11). δ of PIL5 is sensitive to the frequency and becomes more liquid-like as the frequency increased. The increase in the rate of G'' is apparent in Figure S11 (see blue curve). As the slope of the tangent function rapidly increases between 45 degrees and 90 degrees, the liquid nature of the hexyl IL quickly becomes more pronounced. δ for PIL6 maintains a constant 90 degrees value, which is characteristic of a liquid-like material. This reflects a larger G'' value than G' value. The data beyond 100 rad/s for PIL6 fluctuates around 90 degrees. Values larger than 90 degrees are the result of the device over correcting whilst attempting to measure δ at high frequencies for a material acting as an ideal liquid. The frequency sweeps were therefore only run between 0.01 rad/s and 100 rad/s for the equally liquid-like monocationic ILs.

A decreasing, shear-thinning trend for η is displayed by both PIL4 and PIL5 (See SI, Figure S11). Starting at a magnitude of around 10^6 Pa.s at 0.1 rad/s, both ILs decrease to 10^4 Pa.s with increasing frequency. PIL5 has a similar slope to its butyl

equivalent however, does not plateau in a similar fashion to the PIL4 (See SI, Figure SI1). As η^* of PIL5 is higher than PIL4 at the beginning of the frequency sweep (angular frequency = 0.1 rad/s), the innate viscosity (η_0) must also be higher. However, the difference in values between the two ILs is minimal. PIL6 displays frequency independence and lingers around 10 Pa.s throughout the experiment.

As the anion is exchanged from Cl^- to PF_6^- , SbF_6^- , POA^- , or NTf_2^- for the $(\text{Hex})_3\text{P}(\text{Dec})\text{P}(\text{Hex})_3$ system, the IL became more liquid-like (See SI, Figure SI3). The G' and G'' values were 6 orders of magnitude lower for PIL7 and PIL8 than PIL5 and as much as 7 orders of magnitude for G'' of PIL10. A strong dependence on the frequency is observed for all anion exchanged ILs. Similarly to PIL1 and PIL2, the G' curve for the PF_6^- , SbF_6^- , POA^- , and NTf_2^- IL compositions has a plateau at lower angular frequencies and increases above 1 rad/s (See SI, Figure SI3). A linear G'' curve is seen for the four fluorinated ILs unlike the behavior observed with phosphonium ILs coordinated to chloride ion. Once the size of the anion is larger than a chloride ion, the electrostatic interaction is dramatically compromised. The significant size difference between PF_6^- or SbF_6^- compared to Cl^- has an important role in the loss of material properties. The large G' and G'' of PIL5 is due to the strength of the electrostatic interaction with the introduction of bulky anions. The G' , G'' and η^* of PIL7 consistently maintains slightly higher values than PIL8 (See SI, Figure SI3). The ILs with fluorinated anions possess frequency-independent δ trends and η^* trends, which are consistent with typical ideal viscous behavior with no yield point. For example, η^* of PIL10 is an order of magnitude lower than that of the PF_6^- , SbF_6^- , and POA^- analogs. Similarly to the monocationic ILs, there is a significant amount of noise in the δ and η^* values due to instrument limitations and thus only the results below 100 rad/s are reported.

Despite the differences in the molecular composition of each of the anions, the rheological behavior of OA^- , POA^- , DS^- , and DOSS^- was the same, when complexed with $[(\text{But})_3\text{P}(\text{Dec})\text{P}(\text{But})_3]$. The general shape of the curves in all four graphs mirror those of PIL7 and PIL8 (See SI, Figure SI3). The graph of G' as a function of frequency follows a very gradual 'S-curve' with an inflection point beyond the tested frequency while all of the G'' curves are yet again linear. This difference in shape of the two moduli is reflected in the δ of the ILs, which follow a 'U-shaped' curve with its minimum between 1-10 rad/s. Among the non-halide anions in this section, PIL11 has the smaller molecular weight anion and the highest η^* at 1Hz despite having a similar alkyl chain length than POA^- . Fluorocarbons are known to have lower viscosities compared to hydrocarbon chains, which is reflected from the frequency sweep, in the constantly lower η^* values of PIL12. In contrast, PIL11 exhibits the highest η^* (See SI, Figure SI4). Interestingly, the ILs containing the sulfate anions (DOSS^- and DS^-) possess the second and third highest η^* (See SI, Figure SI4). Due to the symmetrical geometry of PIL13 compared to the former, the higher η is expected¹¹. Again, G'' of the non-chlorine $[(\text{But})_3\text{P}(\text{Dec})\text{P}(\text{But})_3](\text{X})_2$ ILs is larger than G' throughout the frequency sweep. This difference is more pronounced at lower frequencies while the ILs are able to rearrange to accommodate the mechanical stimulus and to maintain a constant G' value. With increasing frequency, the

material becomes more rigid with respect to the applied forces and an increase in the moduli is thus observed.

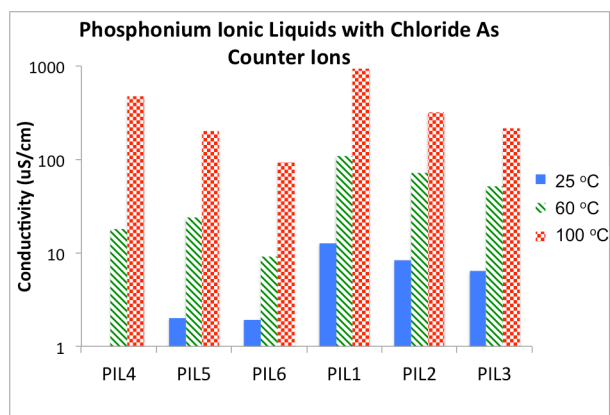


Figure 4. Conductivity values of the phosphonium ionic liquids samples with a chloride counterion.

Conductive properties

Given the interesting rheological properties displayed by the monocationic and dicationic phosphonium ILs, we subsequently investigated their conductivity properties for possible electrochemical applications. At 25 °C, 60 °C, and 100 °C, the monocationic ILs consistently conducted more than their dicationic counterparts (Figure 4, 5, and see SI, Figure SI8). When comparing the monocationic and dicationic chloride ILs with similar side alkyl chains, the conductivity values of the PIL1, PIL2, and PIL3 are an order of magnitude higher than their dicationic counterparts at the same temperature. Only PIL1 is able to attain around 1mS/cm conductivity at 100 °C, a magnitude lower than the current electrolytes used (~10 mS/cm).⁴¹ As both PIL4 and PIL5 are solids at room temperature, the conductivity values are barely detectable in our experiments.

The monocationic phosphonium chlorides possess a sufficiently low η that contributes to their observed higher conductivity values. Figure SI8 shows that dicationic PIL7, PIL8,

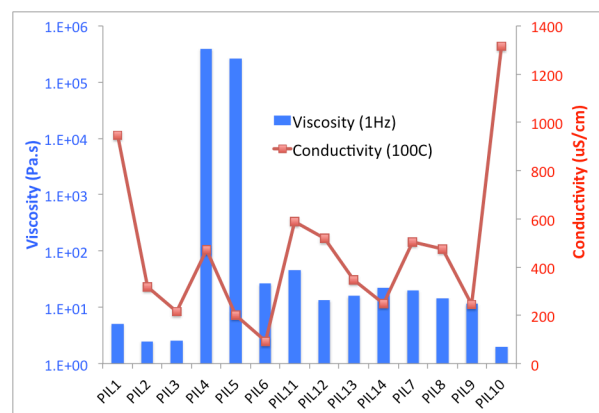


Figure 5. Comparison of viscosity values at 1 Hz and conductivity values at 100 °C of monocationic and dicationic samples. The conductivity value for 1HexBF₄ has been included to show the effect of anion on monocationic samples.

PIL9, PIL11, PIL12, PIL13, and PIL14 achieve higher conductivity values than their halide analog below 60 °C and that

PIL10 is the most conductive at 25, 60, and 100 °C. Relative to each other, negligible conductivity values difference are seen between butyl POA⁻, OA⁻, DS⁻, and DOSS⁻ materials. PIL14 has a slightly lower conductivity value at all three temperatures probably due to the bulky shape of the DOSS⁻ anions, making it less mobile than the other anions (See SI, Figure SI8). The conductivity of PIL12 is very similar to its butyl analog, showing little chain length dependence around the phosphonium. PIL10 conducts almost 20 times more than its chloride analog at 25 °C. Substituting the chloride anion with the bulkier NTf₂⁻ anion reduced the η value by 10⁵ times (2 Pa.s), thus making the ions more mobile in PIL10. In order to compare the conductivity of a monocationic IL with a non-chloride anion, the conductivity of (Hex)₃P(Dec)(BF₄)⁻ was studied (See SI, Figure SI8). This IL has a higher conductivity value than its chloride counterpart at all three temperatures due to the delocalized charge on the anion that affords a fluid IL, which in turn allows for higher ion mobility and therefore higher conductivity.

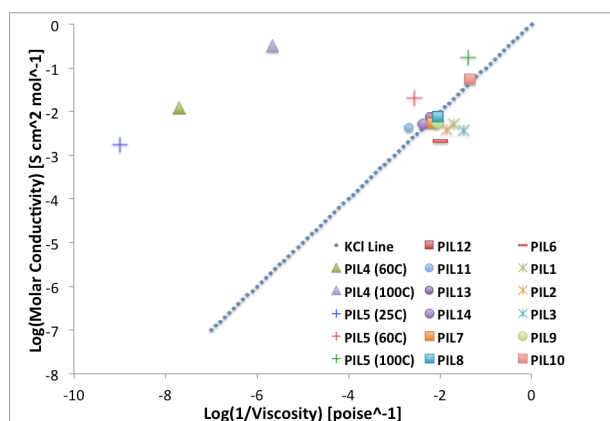


Figure 6. Walden plot of the phosphonium ionic liquids at 25 °C. Data at 25, 60, and 100 °C for PIL4 and PIL5 are included above.

Walden plot

Finally, a Walden Plot was constructed with the zero shear viscosities at 1 Hz and conductivity values at 25 °C for all of the ILs (Figure 6). As the zero shear viscosity values for PIL4 and PIL5, the dicationic chloride ILs, at 60 and 100 °C were not available, the complex viscosity values at 1 Hz were used to provide an approximate trend of the sample ionicity. Often, ILs have values that have a 1:1 proportionality between the logarithm of the fluidity (the inverse of η) and the logarithm of the molar conductivity. While most of the data points lie along the dilute KCl line, agreeing well with the Walden rule (the product of molar conductivity and η of the ions in a solution being constant regardless of the solvent), few of the ILs with the chloride as the counterion lie below the unity line. This deviation of the monocationic species from the unity line agrees with the study reported by MacFarlane *et al.*⁴² At a certain η value, these monocationic ILs are unable to conduct as expected. Their viscosity vs conductivity correlation points lie below the KCl line and display characteristics of liquid ion pairs. The data for PIL4 and PIL5 at 25 °C both lie above the KCl line, in the superionic liquid region. The dimerization of the PIL4 allows for increased

cation-cation correlated motions, causing the sample, together with the PIL5, to lie in the superionic liquid region. This behavior did not follow the trend for the other ILs thus, the test was repeated at other temperatures. As the temperature is increased from 25 °C to 100 °C, the data points for PIL5 approach the KCl line (Figure 5). The same trend is observed as the temperature is increased from 60 °C to 100 °C for PIL4. The conductivity value for the PIL4 is not available at 25 °C. As the temperature increases, a dramatic drop in η is observed for PIL4 and PIL5 as the IL undergoes a phase transition. Thus, caution must be taken when interpreting this increase in ion mobility that is more rapid than the increase in the conductivity. The difference in behavior between the PIL4, PIL5, and the octyl equivalent, PIL6, is again apparent as the last IL obeys the Walden rule. PIL7, PIL10, PIL12, PIL13, and PIL14 lie along the KCl line and display an ideal ionic solution behavior.

Experimental

Synthesis of Phosphonium ILs

Chloride Cl⁻, as anion

All phosphonium chloride ILs were prepared as described in literature using starting materials purchased from Sigma-Aldrich and TCI as highest purity grade.² Dichlorodecane and trialkyl phosphines (1:2 mole ratio for the dicationic ILs and 1:1 for the monocation ILs) were combined together in a glass pressure vessel inside a dry box to minimize oxidation. The mixture was vigorously stirred at 140 °C for 24 hours, the remaining starting materials were removed under vacuum at 140 °C to yield the phosphonium chloride ILs. The products were characterized using ¹H, ¹³C, and ³¹P NMR spectroscopy (Varian 500 MHz, 400 MHz, and 300 MHz), electro-spray mass spectrometry (Agilent Single-Quad LC/MSD VL), differential scanning calorimetry (TA Q100 DSC), and thermal gravimetric analysis (TA Q50 TGA).

Hexafluorophosphate PF₆⁻ and Hexafluoroantimonate SbF₆⁻, as anions

Silver salts with the desired anion were purchased from either Sigma-Aldrich or Strem Chemicals. The silver salt (2.56 mmol) was added to a flask inside a dry box while the chloride ionic liquid (1.28 mmol for the dicationic, 2.56 mmol for the monocationic) was dried under vacuum at 80 °C in a separate flask to ensure minimal hydration. The ionic liquid was then dissolved in 15 mL of anhydrous dichloromethane and added dropwise into the flask containing the silver salt. The solution was stirred for 24 hours at room temperature, under nitrogen with the flask wrapped in aluminum foil. The silver chloride precipitate was filtered out and the supernatant was extracted with a small amount of water until no precipitant was seen when the aqueous phase was tested in silver nitrate. Activated carbon was then added to the organic phase and the solution was further stirred for 24 hours. The activated carbon was then filtered on silica and neutral alumina. Finally, the dichloromethane was removed on the rotavapor and the IL further dried under vacuum. The material was characterized with the same analytical techniques mentioned above.

Perfluorooctanoate POA⁻, as anion

The acid form of the desired anion (6.5 mmol) was combined with PIL4 or PIL5 (3.2 mmol) at a 1:1 charge ratio. 30 mL of anhydrous acetonitrile was added to the flask and the solution was rapidly stirred overnight at 70 °C. The solvent and byproducts were then evaporated under vacuum at 35 °C to yield the desired ILs.

Bis(trifluoromethane)sulfonimide NTf₂⁻, as anion

Lithium bis(trifluoromethane)sulfonimide (6.5 mmol) was combined with PIL5 (3.2 mmol) at a 1:1 charge ratio. 20 mL of water was added to the flask and the solution was rapidly stirred overnight at 45 °C. The solution was extracted with dichloromethane (x3), then the solvents were evaporated under reduced pressure to yield the desired IL.

Dodecyl sulfate DS⁻ and dioctyl sulfosuccinate DOSS⁻, as anion

Either sodium dodecyl sulfate (SDS) or sodium dioctyl sulfosuccinate (6.5 mmol) was dissolved with PIL4 (3.2 mmol) in 40 mL of anhydrous chloroform and rapidly stirred overnight under reflux. The solution was then cooled to room temperature and the dodecyl sulfate was extracted with water. The chloroform was removed from the dioctyl sulfosuccinate solution and the product was redissolved in diethyl ether. The sodium chloride that precipitated out was removed by filtration before the solution was extracted with water. All solvents were evaporated under reduced pressure and the ILs were dried overnight under vacuum. Both phases were verified by ¹H NMR of the ionic liquid in the organic phase and absence of any SDS in the aqueous phase for PIL13.

Octanoate OA⁻, as anion

Caprylic acid (6.4 mmol) was combined with PIL4 (3.2 mmol) in the presence of 20 mL of methanol and stirred overnight at 60 °C. The hydrochloric acid and methanol were removed on the rotavap and then the desired IL was further dried under vacuum. ¹H NMR spectra in deuterated chloroform and dimethylsulfoxide confirmed the presence of both ions, and the absence of the carboxylic acid's proton, respectively.

Rheometrical procedure

All tests were performed using an AR 1000 Controlled-strain rheometer from TA instruments with various flat plates. ILs (1 g) were dried under high vacuum at 100 °C in a flask until consistent baseline dryness was observed on the barometer. The materials were then stored in a parafilm sealed vial at room temperature. All of the frequency sweep tests were performed with the rheometer at room temperature in an enclose space in the present of Dririte. 8 mm steel and 40 mm aluminum parallel plates were used for the testing, depending on the modulus range.

In order to determine the parameters for testing, the following tests were performed: oscillatory stress sweep for a pseudo-linear viscoelastic region (LVR) determination and oscillatory time sweep for conditioning parameters (equilibration time and preshear value) determination. Erasing the solidification history of the ILs was achieved through the preshear and some ILs were melted for mounting between the two plates thus, the equilibration time determination was necessary. The oscillatory

stress sweep was repeated with the determined conditioning values to obtain the LVR. Subsequent tests were run only in the LVR. Frequency sweeps were performed to obtain the storage modulus (G'), loss modulus (G''), complex viscosity (η*), and the phase lag, delta (δ) values.

Thermal gravimetric analysis (TGA)

The thermal stability of the ILs used in this study was analyzed using a TA Instruments Q50 TGA. The ILs were tested over temperature range from room temperature up to 500 °C at 20 °C/min with constant air flow. The decomposition temperatures (T_d) presented in Table 1 and Figure SI5 were calculated using the step tangent method.⁴² The T_d values are slightly lower than those reported for trihexyltetradecylphosphonium chloride and tetrabutylphosphonium chloride although they were obtained in a dinitrogen environment. As the decomposition curves for all ILs tested did not show any evidence of water loss, it can be speculated that the air flow was sufficient in protecting the ILs from significant wetting from the moisture in the atmosphere. It is also possible that the sensitivity of the instrument was not able to register the small amount of water that may have coated the surface of the IL during testing.⁴³

Differential scanning calorimetry (DSC)

The phase transitions of the ILs in this study were observed using a TA Instrument Q100. The samples were prepared in a hermetically sealed aluminum pan and subjected to cyclical temperature ramps of 10 °C/min heating and 20 °C/min cooling between 100 and 150 °C. The analysis of the phase transitions was conducted with TA Instruments Universal Analysis and the values are presented in Table 1.

Conductivity measurements

The conductivity of the ILs were measured on a Consort K912 model. The samples were dried under high vacuum at 100 °C in a vial until consistent baseline dryness was observed by an equilibrated barometer reading. Each sample was transferred into a 4mL vial and placed in a heat block. With the probe completely immersed in the ionic liquid, the temperature was slowly ramped from room temperature up to 100 °C and back down over a period of 3 hours.

Density measurements

The density values of the ILs were measured using a Mettler Toledo DA-110 Handheld Portable Gravity Meter. The samples were dried under high vacuum at 100 °C in a vial until consistent baseline dryness was observed by an equilibrated barometer reading. Each sample was test 3 times at room temperature and the average value was used for the construction of the Walden Plot. Only slight differences were seen between density values as the temperature was increased to 100 °C.

Conclusion

A series of phosphonium based ILs are described with varying alkyl side chain length, number of cationic charge, anion size, and anions with fluorocarbon or hydrocarbon chains, sulfate esters and carboxylate groups. By varying the composition of the phosphonium (monocationic vs dicationic) IL and partnering it

with a particular anion, a specific set of thermal, rheological, and conductive properties can be obtained. For example, the glass transition temperature can be varied from -13 to -68 °C. The [(But)₃P(Dec)P(But)₃] sample with the perfluorooctanoate anion (PIL12) possessing the highest the T_g value (-13 °C) while the corresponding dicationic hexyl phosphonium ionic liquid with the bis(trifluoromethane)sulfonamide (PIL10) possessing the lowest (-68 °C). The glass transition temperature for monocationic phosphonium chloride ILs are relatively insensitive to alkyl chain length difference unlike the dicationic ILs. The dicationic phosphonium chlorides are room temperature ILs at 25 °C only when the alkyl side chain is longer than eight carbons *e.g., PIL3) whereas all of the monocationic phosphonium chlorides are liquids at 25 °C. For the decomposition temperature, an alkyl side chain length dependence is observed for the dicationic chloride ILs while only a modest dependence is seen for the monocationic chloride counterparts. All of the samples exhibit initial decomposition temperatures above 150 °C. The octanoate and its fluorinated analog possess the lowest decomposition temperature and the dicationic hexyl sample bis(trifluoromethane)sulfonimide possesses the highest (> 370 °C).

Frequency sweep curves for dicationic phosphonium chloride ILs show that varying the alkyl side chain length led to a large change in rheological properties of the materials when more than six carbons per chain surrounded the phosphorous atom. The lower η values measured for the monocationic species reflect the reduced number of electrostatic interactions between the cation and chloride ion compared to its dicationic equivalent. This trend is also observed for the conductivity values where, in general, the monocationic species are more conductive compared to the dicationic chloride analogs. The former can display ion pairing while the latter can act as superionic liquids. Substituting the chloride with a larger anion, lengthening the alkyl chain beyond hexyl for the dicationic chloride samples, increasing the temperature, or reducing the cationic charge from two to one for the chloride samples results in a dramatic loss in electrostatic interaction as seen in the Walden Plot by a sudden switch to ideal ionic solution behavior. A conductivity value of around 1mS/cm at 100 °C is achieved by some of the IL reported in this study supporting their further development as electrolyte solvents for batteries, with the caveat, that operation must be at an elevated temperature. Fortunately, there are significant needs for such thermally stable electrolyte solvents for batteries used in the automotive, oil and gas recovery, and manufacturing industries. Continued research in this area will afford new materials as well as insight into the relationships between IL composition and physical and chemical properties. Such information is key for meeting current challenges and future ones.

Acknowledgment

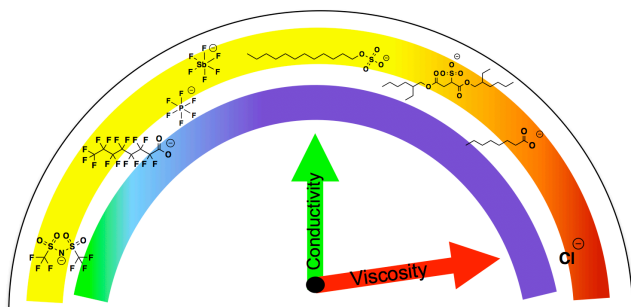
This work was supported in part by National Science Foundation (CHEM 1012464), Advanced Energy Consortium (AEC), and Boston University. The authors thank Dr. Xinrong Lin for helpful discussions.

References

1. P. Wasserscheid and W. Keim, *Angew. Chem.*, 2000, 39, 3772-3789.
2. M. V. Fedorov and A. A. Kornyshev, *Chem. Rev.*, 2014, 114, 2978-3036.
3. T. D. Ho, C. Zhang, L. W. Hantao and J. L. Anderson, *Anal. Chem.*, 2014, 86, 262-285.
4. R. Sharma and R. K. Mahajan, *RSC Advances*, 2014, 4, 748-774.
5. J. Yuan, D. Mecerreyes and M. Antonietti, *Prog. Polym. Sci.*, 2013, 38, 1009-1036.
6. C. Maton, N. De Vos and C. V. Stevens, *Chem. Soc. Rev.*, 2013, 42, 5963-5977.
7. A. Rehman and X. Zeng, *Acc. Chem. Res.*, 2012, 45, 1667-1677.
8. G. Chatel, J. F. B. Pereira, V. Debbeti, H. Wang and R. D. Rogers, *Green Chem.*, 2014, 16, 2051-2083.
9. M. Wathier and M. W. Grinstaff, *J. Am. Chem. Soc.*, 2008, 130, 9648-9649.
10. X. Lin and M. W. Grinstaff, *Isr. J. Chem.*, 2013, 53, 498-510.
11. X. Lin, L. Navailles, F. Nallet and M. W. Grinstaff, *Macromolecules*, 2012, 45, 9500-9506.
12. H. Sakaabe and H. Matsumoto, *Electrochem. Commun.*, 2003, 5, 594-598.
13. F. Zhou, Y. Liang and W. Liu, *Chem. Soc. Rev.*, 2009, 38, 2590-2599.
14. M. A. Navarra, S. Panero and B. Scrosati, *Electrochem. Solid-State Lett.*, 2005, 8, A324-A327.
15. M. A. B. H. Susan, T. Kaneko, A. Noda and M. Watanabe, *J. Am. Chem. Soc.*, 2005, 127, 4976-4983.
16. S. S. Sekhon, J. Park, J. Baek, S. Yim, T. Yang and C. Kim, *Chem. Mater.*, 2010, 22, 803-812.
17. S. Caporali, A. Fossati, A. Lavacchi, I. Perissi, A. Tolstogousov and U. Bardi, *Corros. Sci.*, 2008, 50, 534-539.
18. G. Adamova, R. L. Gardas, M. Nieuwenhuysen, A. V. Puga, L. P. Rebelo, A. J. Robertson and K. R. Seddon, *Dalton Transaction*, 2012, 41, 8316-8332.
19. G. Adamova, R. L. Gardas, L. P. Rebelo, A. J. Robertson and K. R. Seddon, *Dalton Transaction*, 2011, 40, 12750-12764.
20. C. P. Fredlake, J. M. Crosthwaite, D. G. Hert, S. N. V. K. Aki and J. F. Brennecke, *J. Chem. Eng. Data*, 2004, 49, 954-064.
21. J. M. Pringle, J. Golding, C. M. Forsyth, G. B. Deacon, M. Forsyth and D. R. MacFarlane, *J. Mater. Chem.*, 2002, 12, 3475-3480.
22. Z. S. Breitbach and D. W. Armstrong, *Anal. Bioanal. Chem.*, 2008, 390, 1605-1617.
23. F. M. Gaciño, T. Regueira, L. Lugo, M. J. P. Comuñas and J. Fernández, *J. Chem. Eng. Data*, 2011, 56, 4984-4999.
24. S. Seki, T. Kobayashi, Y. Kobayashi, K. Takei, H. Miyashiro, K. Hayamizu, S. Tsuzuki, T. Mitsugi and Y. Umehayashi, *J. Mol. Liq.*, 2010, 152, 9-13.
25. A. Pinkert, K. L. Ang, K. N. Marsh and S. Pang, *Phys. Chem. Chem. Phys.*, 2011, 13, 5136-5143.
26. J. L. Anderson, R. Ding, A. Ellern and D. W. Armstrong, *J. Am. Chem. Soc.*, 2005, 127, 593-604.
27. T. Payagala, J. Huang, Z. S. Breitbach, P. S. Sharma and D. W. Armstrong, *Chem. Mater.*, 2007, 19, 5848-5850.
28. G. Godeau, L. Navailles, F. Nallet, X. Lin, T. J. McIntosh and M. W. Grinstaff, *Macromolecules*, 2012, 45, 2509-2513.
29. K. J. Fraser and D. R. MacFarlane, *Aust. J. Chem.*, 2009, 62, 309-321.
30. J. D. Holbrey and K. R. Seddon, *Journal of the Chemical Society, Dalton Transactions*, 1999, 13, 2133-2139.
31. M. Y. Keating, F. Gao and J. B. Ramsey, *J. Therm. Anal. Calorim.*, 2011, 106, 207-211.
32. L. M. V. Pinheiro, A. R. T. Calado and J. C. R. Reis, *Organica Biomolecular Chemistry*, 2004, 2, 1330-1338.
33. J. G. Huddleston, A. E. Visser, W. M. Reichert, H. D. Willauer, G. A. Broker and R. D. Rogers, *Green Chem.*, 2001, 3, 156-164.
34. H. Ngo, K. LeCompte, L. Hargens and A. B. McEwen, *Thermochim. Acta*, 2000, 97-102.
35. C. Chiappe and D. Pieraccini, *J. Phys. Org. Chem.*, 2005, 18, 275-297.

36. S. Sowmiah, V. Srinivasadesikan, M. C. Tseng and Y. H. Chu, *Molecules*, 2009, 14, 3780-3813.
37. C. Nanjundiah, J. L. Goldman, L. A. Dominey and V. R. Koch, *J. Electrochem. Soc.*, 1988, 135, 2914-2917.
38. K. Y. Jen, G. G. Miller and R. L. Elsenbaumer, *J. Chem. Soc., Chem. Commun.*, 1986, 17, 1346-1347.
39. M. Petkovic, J. L. Ferguson, H. Q. N. Gunaratne, R. Ferreira, M. C. Leitão, K. R. Seddon, L. P. N. Rebelo and C. S. Pereira, *Green Chem.*, 2010, 12, 643-649.
40. M. Anouti, M. Caillon-Caravanier, Y. Dridi, H. Galiano and D. Lemordant, *The Journal of Physical Chemistry B*, 2008, 112.
41. L. Suo, Y. S. Hu, H. Li, M. Armand and L. Chen, *Nat. Commun.*, 2013, 4, 1481.
42. K. J. Fraser, E. I. Izgorodina, M. Forsyth, J. L. Scott and D. R. MacFarlane, *Chem. Commun.*, 2007, DOI: 10.1039/b710014k, 3817-3819.
43. T. Erdmenger, J. Vitz, F. Wiesbrock and U. S. Schubert, *J. Mater. Chem.*, 2008, 18, 5267-5273.

Insert Table of Contents artwork here



20 word text:

Specific thermal, rheological, and conductive properties of phosphonium ionic liquids can be obtained through judicious choice of cation and anion.